

Numerical Simulation and Experimental Study of Ar/CH₄ Coaxial DBD Discharge Characteristics

Siyuan WANG^{a,1}, Peng SONG^a, Huan PEI^b, Qiyu LI^a and Zhibo ZHAO^a

^a School of Mechanical and Electrical Engineering, Dalian Minzu University, China

^b Aerospace Engineering Institute, Shenyang Aerospace University, Shenyang, China

Abstract. This paper established a one-dimensional model of a coaxial dielectric barrier discharge (DBD) with a single dielectric layer covering the high-voltage electrode. The mixture of Ar and a small amount of CH₄ was used as working gas, the influence of different voltage amplitude on the discharge characteristics was studied by 10.0 kHz microsecond pulsed power. The simulation results show that the discharge current curve presents bipolar characteristics with different intensities are generated in a single microsecond pulse period, and the primary discharge is much intense. The discharge current, discharge power can enhance by increasing the discharge voltage amplitude. The equivalent capacitance C_g also increases, the discharge voltage has no significant effect on C_d . In the experiment, it can be observed that the number of discharge filaments in the discharge gap increases with the increase of voltage amplitude, and photoionization is formed near the anode. The result of the current experimental trend is almost the same as the simulated current.

Key words. Microsecond pulse, dielectric barrier discharge, numerical simulation, discharge characteristics

1. Introduction

Non-equilibrium plasma technology has many research and applications in biomedical sterilization[1,2], flow control[3,4], auxiliary combustion[5,6], material surface modification[7,8], and environmental protection[9,10]. Dielectric barrier discharge(DBD) is a non-equilibrium plasma discharge in which an insulating medium is placed between the high-voltage electrode and the cathode[11]. When the high-voltage electrode voltage is high enough, a large amount of plasma will be generated in the discharge gap. Domestic and foreign scholars have carried out many experiments[12,13] and simulation studies[14,15] on the discharge characteristics of DBD under the action of AC power supply. However, with the development of high-frequency power supply and improvement of electrical appliances, the high efficiency and high energy characteristics of the microsecond pulse power supply have gradually become a hot spot for the research and application of plasma[16-18].

¹ Siyuan WANG, School of Mechanical and Electrical Engineering, Dalian Minzu University, No. 18, Liaohe West Road, Economic and Technological Development Zone of Dalian, China; E-mail: 2679952790@qq.com.

In this paper, the discharge voltage curve fitted by the actual voltage data of the microsecond pulse power supply is used as the simulation input voltage to explore the influence of changing the voltage amplitude on the plasma discharge characteristics, the result of the discharge current, discharge power, equivalent capacitance, and electron density, ion number density are specifically analyzed. The simulation results can be referenced in analyzing the discharge characteristics of the Ar/CH₄ coaxial DBD plasma by the microsecond pulsed power. By building an experimental platform, the current results in the circuit are measured, which are similar to the numerical simulation results, and finally, the discharge photos are taken.

2. Simulation Model

2.1. Structure of DBD reactor

The experimental system diagram is shown in figure 1 uses the Keysight 3012T oscilloscope to collect the channel data of the high-frequency power supply and connect the 'I-R' channel to measure the device current. The high-voltage probe model is Keysight N2873A. A digital camera was placed directly in front of the discharger outlet during the experiment to capture the observed illuminate phenomenon.

In this paper, a coaxial dielectric barrier discharge plasma structure with a single dielectric layer covering the high voltage electrode is established. The structure diagram is shown in figure 2. The diameter of the center electrode is 6.5mm, the thickness of the dielectric layer is 1.0mm, and the discharge gap width is 3.0mm. The "Ar/CH₄" mixed gas is injected into the discharge gap, and the outermost layer is the cathode.

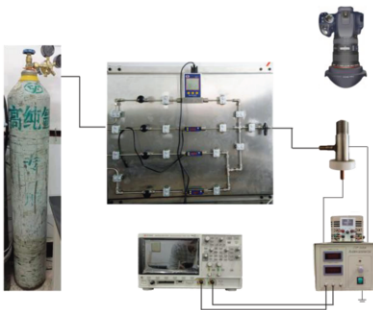


Figure 1. Schematic diagram of the experimental system.

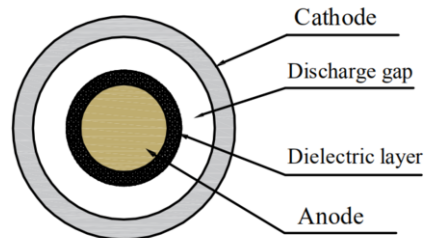


Figure 2. Diagram of coaxial DBD reactor structure.

2.2. Basis of the Model

The mathematical model is a crucial factor for calculation speed and accuracy. Generally, the plasma theory models include particle model (PIC/MCC), fluid model, and hybrid model. Because the fluid model considers the self-consistency problem when analyzing the atmospheric pressure discharge, and the calculation of the model is convenient and fast, this study uses a physical model based on the fluid model.

Equation (1) is Poisson's equation, which is mainly used to solve the electric potential of the plasma and calculate the field distribution of the discharge gap, further

describe the movement of charged particles in the electrostatic field, and calculate the charge.

$$\epsilon_0 \nabla \cdot (\epsilon_r E) = \rho \tag{1}$$

$$\rho = q \left(\sum_{k=1}^N Z_k n_k - n_e \right) \tag{2}$$

The continuity equation of electron density can be expressed as:

$$\frac{\partial}{\partial t}(n_e) + \nabla \cdot \Gamma_e = R_e - (u \cdot \nabla) n_e \tag{3}$$

$$\Gamma_e = -(\mu_e \cdot E) n_e - \nabla(D_e n_e) \tag{4}$$

The energy conservation equation of electron energy density can be expressed as:

$$\frac{\partial}{\partial t}(n_e) + \nabla \cdot \Gamma_e + E \cdot \Gamma_e = R_e - (u \cdot \nabla) n_e \tag{5}$$

$$\Gamma_e = -(\mu_e \cdot E) n_e - \nabla(D_e n_e) \tag{6}$$

The boundary condition equations of the model can be expressed as:

$$\Gamma_e \cdot n = \frac{1}{4} n_e \cdot \left(\frac{8k_b T_e}{\pi m_e} \right)^{1/2} - \alpha_s \sum_i \gamma_i (\Gamma_i \cdot n) + \alpha'_s \mu_e n_e E \tag{7}$$

$$\Gamma_i \cdot n = \frac{1}{4} n_i \cdot \left(\frac{8k_b T_i}{\pi m_i} \right)^{1/2} + \alpha'_s \mu_i n_i E \tag{8}$$

3. Research Results and Analysis

3.1. Analysis of Bipolar Characteristics of Discharge Process

In this research, the microsecond pulse power supply is used, which the frequency is set at 10kHz. The numerical simulation input voltage is based on the actual measured voltage curve and obtained by polynomial fitting.

Figure 3.a shows the actual voltage and fitted voltage curve of 10kV. Figure 3.b shows the corresponding discharge current curve. The discharge current curve has two peaks in a single cycle (T = 100µs). The simulation and experimental current curve results are close.

$$i_g = \left(1 + \frac{C_g}{C_d}\right) i_t - C_g \frac{du_t}{dt} \tag{9}$$

$$u_g = \frac{C_d}{C_d + C_g} u_t - \frac{1}{C_d + C_g} \int_0^t i_g(t) dt \tag{10}$$

$$u_d = \frac{1}{C_d} \int_0^t i_t(t) dt \tag{11}$$

$$i_d = \left(\frac{C_d C_g}{C_d + C_g}\right) \frac{du_t}{dt} \tag{12}$$

According to the equation (9-12), the voltage and current curves of the discharge gap and the dielectric layer are simulated as shown in figure 3.c. It can be seen that the discharge voltage u_t and the dielectric layer voltage u_d are unipolar pulse curves, the dielectric layer voltage u_g is a bipolar curve. The discharge gap current i_g and

displacement current i_d curves both show bipolar characteristics, which means there are two discharge processes in a single cycle: during the voltage rising edge phase u_d and i_d on the dielectric layer rise rapidly, and the voltage u_d of the dielectric layer is much larger than u_g . Then in the falling edge of the voltage ($8\mu s \leq t \leq 16\mu s$), a reverse current is generated, and i_g and i_d increase in the opposite direction. Finally, the discharge extinguishing current gradually decreases, and the peak values in the positive and negative directions of i_g are slightly larger than the total current i_t .

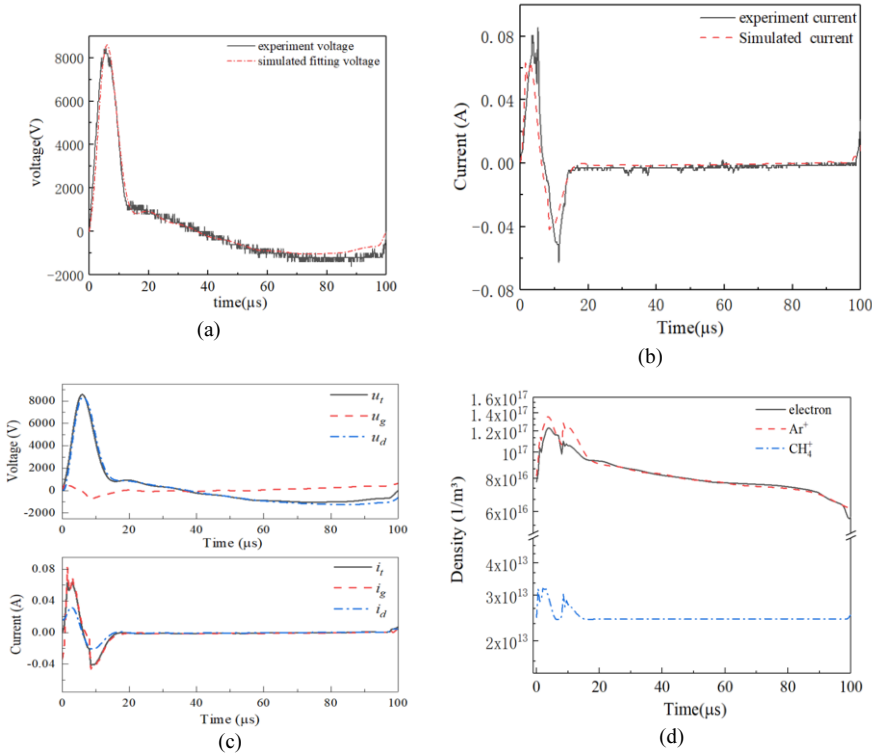


Figure 3. Curve of discharge voltage and discharge current.

Figure 3.d shows the time-varying curves of electron density, Ar⁺ and CH₄⁺ under a voltage of 10kV. During the voltage rise period, the particles move and collide quickly under the electric field, generating many free electrons and ions and reaching the maximum particle value at time $t = 3\mu s$. The maximum electron density is $1.23 \times 10^{17} m^{-3}$, and the maximum Ar⁺ is $1.35 \times 10^{17} m^{-3}$, the maximum value of CH₄⁺ is $3.19 \times 10^{13} m^{-3}$; During the voltage falling period, the current increases in the opposite direction, the number of new products produced is lower.

Figure 4 shows the distribution of electron density, Ar⁺ and CH₄⁺ with time in the discharge gap. At the beginning of the discharge cycle, ionization generates a large number of free electrons, which obtain high energy under the action of an electric field, and collides with gas molecules or atoms. The collision of molecules with the wall causes the emission of secondary electrons, generating more electrons, so the electrons change more drastically near the cathode. With the decrease of the discharge voltage, the intensity of the electric field weakens, and the plasma accumulation near the anode cannot be maintained, which causes the number density of each substance to drop

sharply.

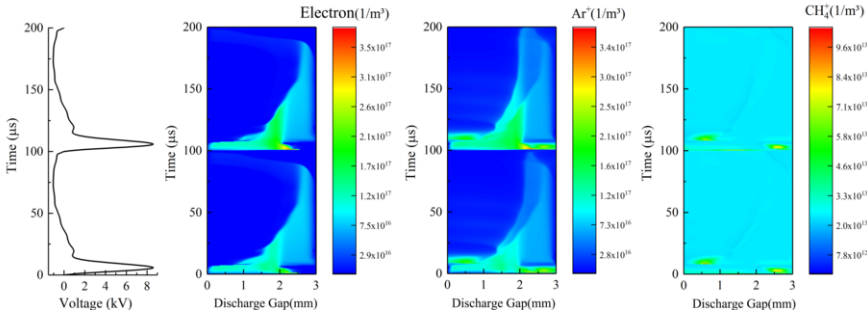


Figure 4. Distribution diagram of electron density, Ar⁺ and CH₄⁺ density.

3.2. The Influence of Voltage Amplitude on Discharge Characteristics

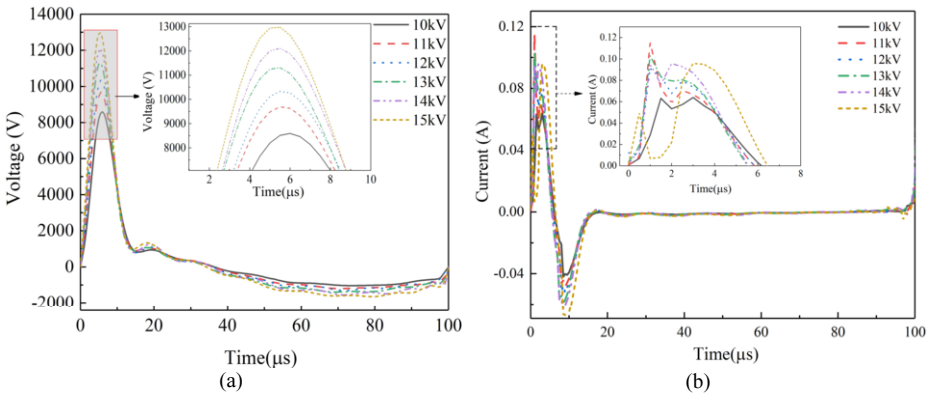
The fitted voltage curve of 10.0~15.0kV is shown in figure 5.a, and the current curve is shown in figure 5.b. It can be seen that as the discharge voltage amplitude increases, the discharge current value becomes larger, which means the DBD discharge is more intense. Draw the Lissajous figure as shown in figure 5.c. According to equation (13), the discharge power by 10~15kV voltage supply is 2.31w, 2.61w, 2.82w, 3.19w, 3.41w, 3.64w, respectively.

$$P = \frac{1}{T} \int_0^T UI dt = \frac{C}{T} \int_0^T U dQ = f \cdot S_L \tag{13}$$

$$\frac{1}{C} = \frac{1}{C_d} + \frac{1}{C_g} \tag{14}$$

$$C_g = \frac{C C_d}{C_d - C} \tag{15}$$

By calculating the slope of the two parallel sides in the Lissajous pattern, the equivalent capacitance C_d of the dielectric layer and the total capacitance C , the equivalent capacitance C_g of the discharge gap is calculated according to equation (15). Figure 5.d shows the curve of C_d , C_g , C with discharge voltage. It can be seen from the figure that C_d is changeless, and C_g gradually increases with the increase of the voltage amplitude. According to equation (14), the total capacitance C also increases with the increase of the voltage amplitude.



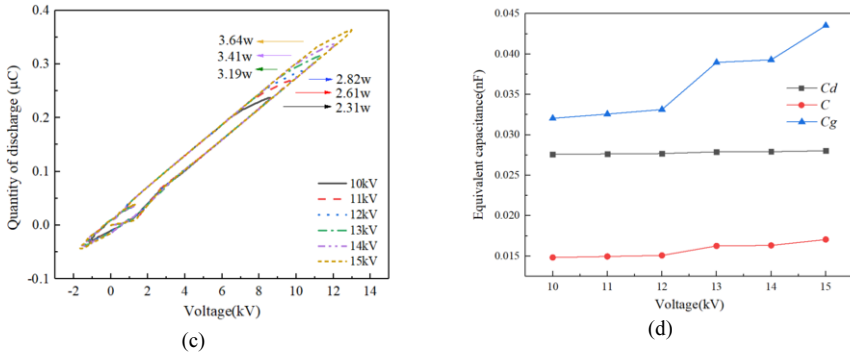


Figure 5. Discharge characteristic curves of different voltage amplitudes.

3.3. Comparison of Numerical Simulation and Experimental Results

The experiment shown in figure 6 is compared with the voltage and current graphs of the numerical simulation. It can be seen that the simulation and experimental results are generally consistent. The discharge current is bipolar, and the discharge current gradually promote with the increase of the discharge voltage.

However, the simulated current reaches its peak time as 1-2μs earlier than the experimental result. There are many irregular spike-like burrs at the peak of the current measured under the experimental conditions. The numerical simulation current results are relatively smooth, which may be caused by the ignorance of the resistance and capacitance in the experimental circuit in the numerical simulation.

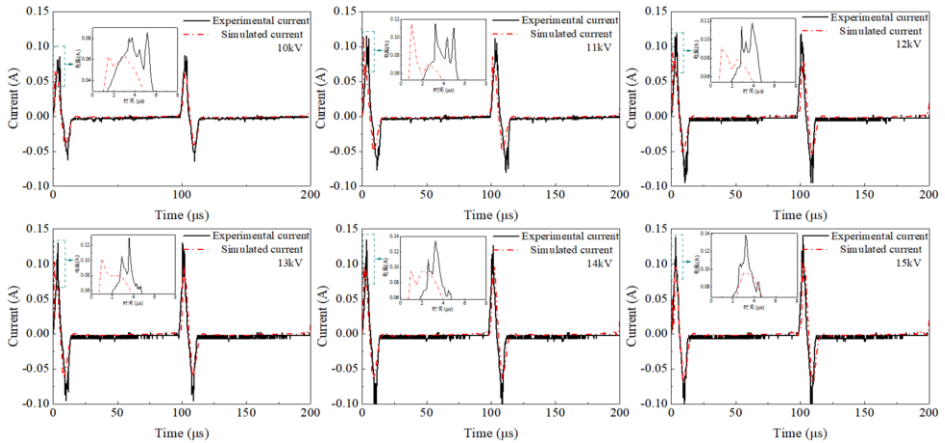


Figure 6. Comparison of 10-15kV voltage experiment and simulation current.

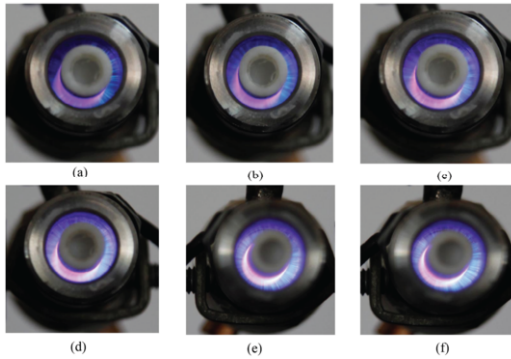


Figure 7. DBD ionization phenomenon of the discharger at 10-15kV.

It can be seen from figure 7 that with the increase of the voltage amplitude, the number of discharge filaments in the discharge gap increases significantly, and the discharge brightness in the gap gradually becomes brighter. The mixed gas is ionized under the applied high-voltage electric field. A large number of free electrons are accelerated from the cathode to the anode under the action of the electric field force. In addition, during the movement, it collides with the remaining mixed gas, and an electron avalanche occurs. With the generation of high-energy photons, photoionization is formed, and the photoionization of the electron avalanche near the anode region is stronger.

4. Conclusion

In this paper, based on the coaxial dielectric barrier discharge plasma reactor, a one-dimensional fluid simulation model is established to study the influence of different voltage amplitudes on the discharge characteristics of DBD, and experiments are carried out. The following conclusions are made:

- (1) The microsecond pulse power supply can effectively generate plasma. The primary discharge process occurs at the rising and falling edges of the pulse voltage, and the total current is bipolar. The changing trend of the number density of the plasma product is consistent with the changing trend of the total current over time.
- (2) By increasing the amplitude of the external power supply voltage, the plasma discharge intensity can be changed, the reactor power can be increased. Changing the voltage amplitude has little effect on the equivalent capacitance C_d . Both the discharge gap capacitance C_g and the total capacitance C increase with the discharge voltage amplitude.
- (3) As the voltage amplitude increases, the number of discharge filaments in the discharge gap increases significantly, the discharge brightness on the central anode gradually becomes illumination, and the photoionization near the anode area becomes bright.

Acknowledgments

This research is supported by the National Natural Science Foundation of China (Nos. 51509035).

Reference

- [1] Cheng H, Liu X, Lu X, et al. 2016 Numerical study on propagation mechanism and bio-medicine applications of plasma jet. *J. High Voltage*, **1(2)**: 62-73.
- [2] Marsit N M, Sidney L E, Branch M J, et al. 2017 Terminal sterilization: Conventional methods versus emerging cold atmospheric pressure plasma technology for non-viable biological tissues. *J. Plasma Processes and Polymers*, **14(7)**.
- [3] Niu Z-G, Liu J, Liang H, et al. 2019 Flying wing flow separation control by microsecond pulsed dielectric barrier discharge at high Reynolds number. *J. Aip Advances*, **9(12)**.
- [4] Wan G, Jin Y, Li H, et al. 2016 Study on Free Surface and Channel Flow Induced by Low Temperature Plasma via Lattice Boltzmann Method. *J. Plasma Science & Technology*, **18(3)**: 331-336.
- [5] Ju Y, Sun W 2015 Plasma assisted combustion: Dynamics and chemistry. *J. Progress in Energy and Combustion Science*, **48**: 21-83.
- [6] Starikovskiy A, Aleksandrov N 2013 Plasma-assisted ignition and combustion. *J. Progress in Energy and Combustion Science*, **39(1)**: 61-110.
- [7] Cimerman R, Cibikova M, Satrapinskyy L, et al. 2020 The Effect of Packing Material Properties on Tars Removal by Plasma Catalysis. *J. Catalysts*, **10(12)**.
- [8] Wang J, Chen X, Reis R, et al. 2018 Plasma Modification and Synthesis of Membrane Materials-A Mechanistic Review. *J. Membranes*, **8(3)**.
- [9] Zhou R, Zhou R, Prasad K, et al. 2018 Cold atmospheric plasma activated water as a prospective disinfectant: the crucial role of peroxyxynitrite. *J. Green Chemistry*, **20(23)**.
- [10] Niedzwiedz I, Wasko A, Pawlat J, et al. 2019 The State of Research on Antimicrobial Activity of Cold Plasma. *J. Polish Journal of Microbiology*, **68(2)**: 153-164.
- [11] Kogelschatz U 2003 Dielectric-Barrier Discharges: Their History, Discharge Physics, and Industrial Applications. *J. Plasma Chemistry and Plasma Processing*, **23(1)**.
- [12] Yao C, Chen S, Wang S, et al. 2018 Characteristics of atmospheric Ar/NH₃ DBD and its comparison with He/N₂ DBD. *J. Journal of Physics D-Applied Physics*, **51(22)**.
- [13] Yaoge L, Yanpeng H, Bin Z 2013 Temporally-Resolved Emission Spectroscopic Diagnostics of the Atmospheric Pressure Glow Discharge in Helium. *J. Plasma Science and Technology*, **15(9)**.
- [14] Zhang Y H, Ning W J, Dai D, et al. 2019 Influence of nitrogen impurities on the characteristics of a patterned helium dielectric barrier discharge at atmospheric pressure. *J. Plasma Science and Technology*, **21(07)**: 23-37.
- [15] Wang L, Huang X, Chen J, et al. 2017 Simulated and experimental studies on the array dielectric barrier discharge of water electrodes. *J. Plasma Science & Technology*, **19(3)**.
- [16] Zhang X, Lee B J, Im H G, et al. 2016 Ozone Production With Dielectric Barrier Discharge: Effects of Power Source and Humidity. *J. Ieee Transactions on Plasma Science*, **44(10)**: 2288-2296.
- [17] Qiu X-D, Su J-C, Zhang Y, et al. 2018 Investigation of Vacuum Gap Breakdown under Microsecond Pulses. *J. Ieee Transactions on Dielectrics and Electrical Insulation*, **25(6)**: 2040-2048.
- [18] Mi Y, Liu L, Gui L, et al. 2019 Effect of frequency of microsecond pulsed electric field on orientation of boron nitride nanosheets and thermal conductivity of epoxy resin-based composites. *J. Journal of Applied Physics*, **126(20)**.